RNA silencing response in chloroplast-replicating viroid siRNA biogenesis in plants

Phytopathology Research

RESEARCH

Open Access

RNA silencing response in chloroplast-replicating viroid siRNA biogenesis in plants

Pengcheng Zhang[1,2*], Xinlian Zhang[3], Atef M. Mohamed[4], Leizhen Wang[1], José-Antonio Daròs[5], Shifang Li[6], Mahmut Tör[2] and Yiguo Hong[1,2*]

Abstract

RNA silencing represents a cellular regulatory and defence mechanism in eukaryotes across kingdoms. In plants, a combined functionality of *DCL2* and *DCL3* is crucial for their synergistic defence against whilst *DCL4* is required for nucleus-replicating viroid. However, how RNA silencing targets and fights against chloroplast-replicating viroid remains unknown. Here, utilizing eggplant latent viroid (ELVd), a chloroplast replicating viroid and a suite of transgenic *Nicotiana benthamiana* RNAi lines *RDR6i* and *DCLsi*, we reveal that *DCLs* and *RDR6* partake a dynamic RNA silencing-mediated response to ELVd infection. *DCL1i*, *DCL2i*, *DCL3i*, and *DCL4i* enhance, whilst *RDR6i* seems to have little impact on, ELVd accumulation. Through small RNA profiling, we unravel that *DCL2* plays an essential role in generating 22 nt ELVd siRNA. *DCL3* is functionally redundant to *DCL2* and targets ELVd for biogenesis of 24 nt chloroplastic viroid siRNA (cvd-siRNA) in the absence of *DCL2*. *DCL4* accounts for the less abundant 21 nt cvd-siRNA production. *DCL1* does not contribute to the cvd-siRNA biogenesis. However, ELVd infection reduces DCL1-processed miRNAs in both wild-type and RNAi plants, suggesting that *DCL1* might indirectly participate in protection of plants from ELVd attack. RDR6 imposes no influence on the 21–24 nt size profile of cvd-siRNA, but affects cvd-siRNA abundance at the late stage of ELVd infection. Our results also demonstrate that a different processing might be responsible to produce chloroplastic small RNAs (csRNAs) in chloroplasts. The dynamic changes of csRNAs during ELVd infection suggest that csRNAs might be of biological relevance to chloroplastic viroid-host plant interactions.

Keywords Chloroplast-replicative viroid, *DCLs*, ELVd, RNA silencing, vd-siRNA, Viroid-plant interactions

*Correspondence:
Pengcheng Zhang
zpc604@126.com
Yiguo Hong
y.hong@worc.ac.uk
[1] Research Centre for Plant RNA Signaling and Zhejiang Provincial Key Laboratory for Genetic Improvement and Quality Control of Medicinal Plants, College of Life and Environmental Sciences, Hangzhou Normal University, Hangzhou 311121, China
[2] School of Science and the Environment, University of Worcester, Worcester WR2 6AJ, UK
[3] Department of Family Medicine and Public Health, Division of Biostatistics & Bioinformatics, University of California San Diego, La Jolla, San Diego, CA 92093, USA
[4] Department of Botany, Faculty of Agriculture, Fayoum University, Fayoum 63514, Egypt
[5] Instituto de Biologia Molecular y Celular de Plantas (CSIC-Universitat Politècnica de València), Avenida de los Naranjos S/N, 46022 Valencia, Spain
[6] Environment and Plant Protection Institute, Chinese Academy of Tropical Agricultural Sciences, Haikou 571101, China

Background

RNA silencing represents a cellular regulatory and defence mechanism in eukaryotes across kingdoms (Baulcombe 2004; Sarkies and Miska 2014; Wang et al. 2022). In plants, single-stranded RNA (ssRNA) can form double-stranded (ds) structures via intramolecular base-pairing or be converted into dsRNA by RNA-dependent RNA polymerases (RDRs) such as RDR6. DICER-LIKE (DCL) endonucleases DCL4, DCL2, and DCL3 then slice dsRNA into small interfering RNA (siRNA) of 21, 22, and 24 nucleotides (nt), respectively. Subsequently, the guide-strand of siRNA and ARGONAUTEs (AGOs), for instance AGO1/2/4, along with other cellular factors form the RNA-induced silencing complex (RISC), which targets specific RNA for cleavage or homologous DNA for RNA-directed DNA methylation, leading to post-transcriptional or transcriptional gene silencing (Sarkies and Miska 2014; Zhang et al. 2019; Wang et al. 2022). RNA silencing can also be triggered by microRNA (miRNA). miRNA is processed from pre-microRNA by DCL1 and causes miRNA-mediated mRNA degradation or arrest of mRNA translation. In plants, RNA silencing represents a potent innate defence against pathogens including viruses (Shi et al. 2008; Aliyari and Ding 2009; Csorba et al. 2015). Indeed, such cellular defence employs DCLs to process plant virus RNAs into viral siRNAs (vsiRNAs). For instance, DCL4 and its cognate 21 nt vsiRNA are essential in the first antiviral frontier of intracellular RNA silencing, whilst DCL2 likely along with DCL2-processed 22 nt vsiRNAs are mainly involved in defensive intercellular silencing (Qin et al. 2017). DCL3 and 24 nt vsiRNA as well as DCL1 and microRNAs also play an important role in combating DNA viruses in plants (Blevins et al. 2006; Aregger et al. 2012).

Viroids are a group of plant pathogens that consist of a non-encapsidated, non-coding, circular ssRNA of 246–434 nt in size (Di Serio et al. 2014; Hammond and Kovalskaya 2014; Hadidi et al. 2017; Adkar-Purushothama and Perreault 2020). They are classified into two families *Pospiviroidae* and *Avsunviroidae*, members of which such as potato spindle tube viroid (PSTVd) and avocado sunblotch viroid (ASBVd) replicate either in the nucleus or chloroplast of host cells, respectively (Flores et al. 2005; Rao and Kalantidis 2015; Hadidi et al. 2017). Impact of RNA silencing on viroids are complex although both nucleus- and chloroplast-replicating viroids can be targeted by RNA silencing (Wang et al. 2004; Bolduc et al. 2010; Dalakouras et al. 2015; Katsarou et al. 2016). Intriguingly, *DCL4* is found to be required for establishment of efficient PSTVd infection of plants since PSTVd accumulates less in *Nicotiana benthamiana dcl4* mutants than in wild-type plants (Dadami et al. 2013). Moreover, both *DCL2* and *DCL3* are crucial in their synergistic defence against PSTVd, and perhaps other nucleus-replicating pospiviroids (Katsarou et al. 2016). Specific 21–24 nt viroid siRNAs (vd-siRNAs) are also profiled for several nucleus- and chloroplast-replicating viroids (Martínez de Alba et al. 2002; Martin et al. 2007; Di Serio et al. 2009; St-Pierre et al. 2009; Bolduc et al. 2010; Martinez et al. 2010; Zhang et al. 2014; Jiang et al. 2019). Pospiviroids may have co-evolved with hosts to be primarily targeted by DCL4 and its cognate 21 nt vd-siRNA, which are less detrimental to viroid infectivity, to avoid the more potent anti-viroid DCL2-DCL3 (22 and 24 nt vd-siRNA) pathways (Katsarou et al. 2016). However, how RNA silencing machinery targets and fights against chloroplastic avsunviroids remains unknown (Martínez de Alba et al. 2002; Di Serio et al. 2009).

To address this question, we utilized eggplant latent viroid (ELVd), a representative member of the family *Avsunviroidae* (Fadda et al. 2003; Daròs 2016), and a suite of transgenic *RDR6*- and *DCL*-RNAi *Nicotiana benthamiana* lines (Chen et al. 2018) in the current study. ELVd, the only species in the genus *Elaviroid* in the family *Avsunviroidae* comprises a 332–335 nt circular non-coding ssRNA genome. ELVd replicates through a rolling-circle mechanism in which RNA strands of both sense (+) and complementary (−) polarities exist in infected cells (Molina-Serrano et al. 2007; Martínez et al. 2009; Nohales et al. 2012). ELVd also contains hammerhead ribozymes in both + and -RNA strands (Fadda et al. 2003). It has a very narrow host range and can be transmitted mechanically and by seed. ELVd systemically and latently infect its natural host eggplant (*Solanum melongena* L.) (Daròs 2016). However, ELVd can also establish local infection in *N. benthamiana* and this pathosystem represents an excellent model to investigate intracellular RNA trafficking between cytoplasm and chloroplasts (Gómez and Pallas 2010, 2012; Nohales et al. 2012). Here, using the ELVd – *N. benthamiana* transgenic lines deficient in cellular RNA silencing (Chen et al. 2018), we investigated how *DCLs* and *RDR6* influence biogenesis of chloroplastic vd-siRNA, designated cvd-siRNA hereafter, in plants.

Results

Experimental design – *DCLs* and *RDR6* vs. chloroplast-replicating viroid

In plants, chloroplastic viroids can generate *sui generis* cvd-siRNAs associated with RNA silencing (Martínez de Alba et al. 2002; Di Serio et al. 2009; St-Pierre et al. 2009; Bolduc et al. 2010). However, this is intriguing due to the physical barrier between subcellular compartments in which chloroplastic viroids replicate and RNA silencing machinery operates. Thus, how cytoplasmic RNA silencing targets chloroplastic viroids for cvd-siRNA biogenesis remains unclear. In addition, it is known that small RNAs

(sRNAs) can be derived from mRNAs, rRNAs, tRNAs, and intergenic RNAs encoded by the chloroplast genome (Wang et al. 2011). These sRNAs are so called chloroplast sRNAs (csRNAs). This brings about another intriguing question on how csRNAs are bio-generated. Indeed, whether csRNAs and cvd-siRNAs are produced through the same cellular RNA silencing apparatus or via distinct sRNA processing/metabolisms is presently unknown. To seek answers to these questions, we exploited transgenic lines in which individual *DCLs* and *RDR6* were knocked-down by RNAi (Chen et al. 2018; Additional file 1: Table S1; Additional file 2: Figure S1) and the fact that ELVd can establish efficient local infection in the non-natural host *N. benthamiana*, and examined the impact of *DCLi* and *RDR6i* on accumulation of cvd-siRNAs and csRNAs that were derived from either ELVd RNA and chloroplast *RbCL* mRNA, respectively.

Compared with wild-type *N. benthamiana* (*Nb*) plants, the corresponding *DCLs* or *RDR6* in each of the independent transgenic lines of *DCL1i, DCL2Ai*, *DCL2Bi*, *DCL3Ai*, *DCL3Bi*, *DCL4Ai*, *DCL4Bi*, and *RDR6i* were specifically targeted, and degradation of *DCLs* or *RDR6* mRNA was evidenced by the elevated reads of specific 21, 22 and 24 nt siRNAs mapped to each gene (Additional file 1: Table S1). Moreover, *RDR6i* had no effect on the size profile of 21, 22 and 24 nt siRNAs, whilst *DCL2i, DCL3i*, and *DCL4i* reduced production of host cellular 22, 24 or 21 nt siRNAs, respectively (Additional file 2: Figure S1a, b). Only *DCL1i* reduced microRNA reads (Additional file 1: Table S2; Additional file 2: Figure S1c). Consistent with our previous reports (Qin et al. 2017; Chen et al. 2018), these data validated the suitability of the *DCLi* and *RDR6i* lines in this study.

Impact of *DCLi* and *RDR6i* on cvd-siRNAs at the early stage of ELVd infection

As demonstrated previously (Gómez and Pallas 2010, 2012; Nohales et al. 2012), we found that ELVd was able to establish local infection in *N. benthamiana* (Fig. 1). Evidently, ELVd RNA was detected by Northern blot in wild-type *Nb*, *DCLi*, and *RDR6i* leaf tissues that were infected by ELVd at days post-inoculation (6-dpi), but not in mock-inoculated *Nb* controls (Fig. 1a). However, due to the limited number of independent samples that could be included in a single gel for Northern analysis, we opted to use RT-PCR to quantify the impact of *DCLi* and *RDR6i* on ELVd RNA accumulation (Fig. 1b). Compared with wild-type *Nb* plants, the average level of ELVd RNA increased by 20%–60% in *DCLi* leaf tissues. An approximate 16% increase in ELVd RNA was also in *RDR6i*, however the difference was not statistically significant (Fig. 1b). These data suggest that *DCL1*, *DCL2*, *DCL3*, and *DCL4*, but not *RDR6*, are involved in plant defense against ELVd at the early stage of infection.

We then assess how *DCLi* and *RDR6i* affect ELVd cvd-siRNA biogenesis. We profiled sRNAs from leaf samples of wild-type *Nb* and RNAi plants that were infected with ELVd at 6 dpi. Total 18–30 nt sRNA profiles (Additional file 2: Figure S2a, b) and the 21, 22 and 24 nt siRNAs that were mapped to individual RNA silencing pathway genes in these ELVd-infected *Nb* and RNAi plants (Additional file 1: Table S3) were similar to those found in healthy controls (Additional file 1: Table S1; Additional file 2: Figure S1a, b). These results indicate that ELVd infection per se did not have obvious influence on the transgenic RNAi knockdown of *DCLs* and *RDR6*.

We then examined the impact of *DCLi* and *RDR6i* on 21, 22 and 24 nt cvd-siRNAs that were specifically mapped to the ELVd 333-nt RNA genome (NC_039241.1; Fig. 2a–l). The size profiles showed several distinct features for ELVd cvd-siRNAs. First, the overall number of sense (+) and antisense (−) 21, 22, and 24 nt cvd-siRNAs was similar among *Nb* (Fig. 2b, c, and l), *RDR6i* (Fig. 2d, l) and all *DCLi* (Fig. 2e–l) plants, although a slight decrease in cvd-siRNAs was seen in *DCL2Ai* (Fig. 2a, l). Compared with each of the ELVd-infected plants, the number of cvd-siRNAs in healthy *Nb* control was almost none (Fig. 2a, l). Second, in ELVd-infected *Nb* plants, the most and least abundant cvd-siRNAs were 22 and 21 nt in length, respectively, and the 24 nt cvd-siRNAs in between (Fig. 2b, c, and l). Reads of 23 nt sRNA were constantly low among all infected plants and possessed no specific association with *RDR6* or any of *DCLs*. Third, the size profiles of 21, 22, and 24 nt cvd-siRNAs and their actual reads were found to be similar among *Nb*, *RDR6i, DCL1i*, *DCL4Ai*, and *DCL4Bi* plants (Fig. 2b–e and j–l), indicating that *RDR6*, *DCL1*, and *DCL4* are not particularly involved in cvd-siRNA biogenesis at the early stage of ELVd infection. Fourth, in *DCL2Ai* and *DCL2Bi*, ELVd 22 nt cvd-siRNAs reduced to extremely low level, but the 24 nt cvd-siRNAs increased whilst the 21 nt cvd-siRNAs also decreased to a less extent at 6 dpi (Fig. 2f, g, and l). However, locations of any given 21, 22, or 24 nt cvd-siRNAs that were mapped to the ELVd genome remained unchanged (Fig. 3a–k). Thus, *DCLi* and *RDR6i* seem to impose no obvious influence on distribution of 21, 22, and 24 nt cvd-siRNAs across both ± RNA strands of the ELVd genome (Fig. 3a–k).

Impact of *DCLi* and *RDR6i* on cvd-siRNA at the later stage of ELVd infection

In a similar experimental setting, we detected ELVd RNA and profiled sRNAs from leaf samples of wild-type *Nb* and RNAi plants at 14 dpi, a later stage of ELVd infection. Like at the early infection stage, a

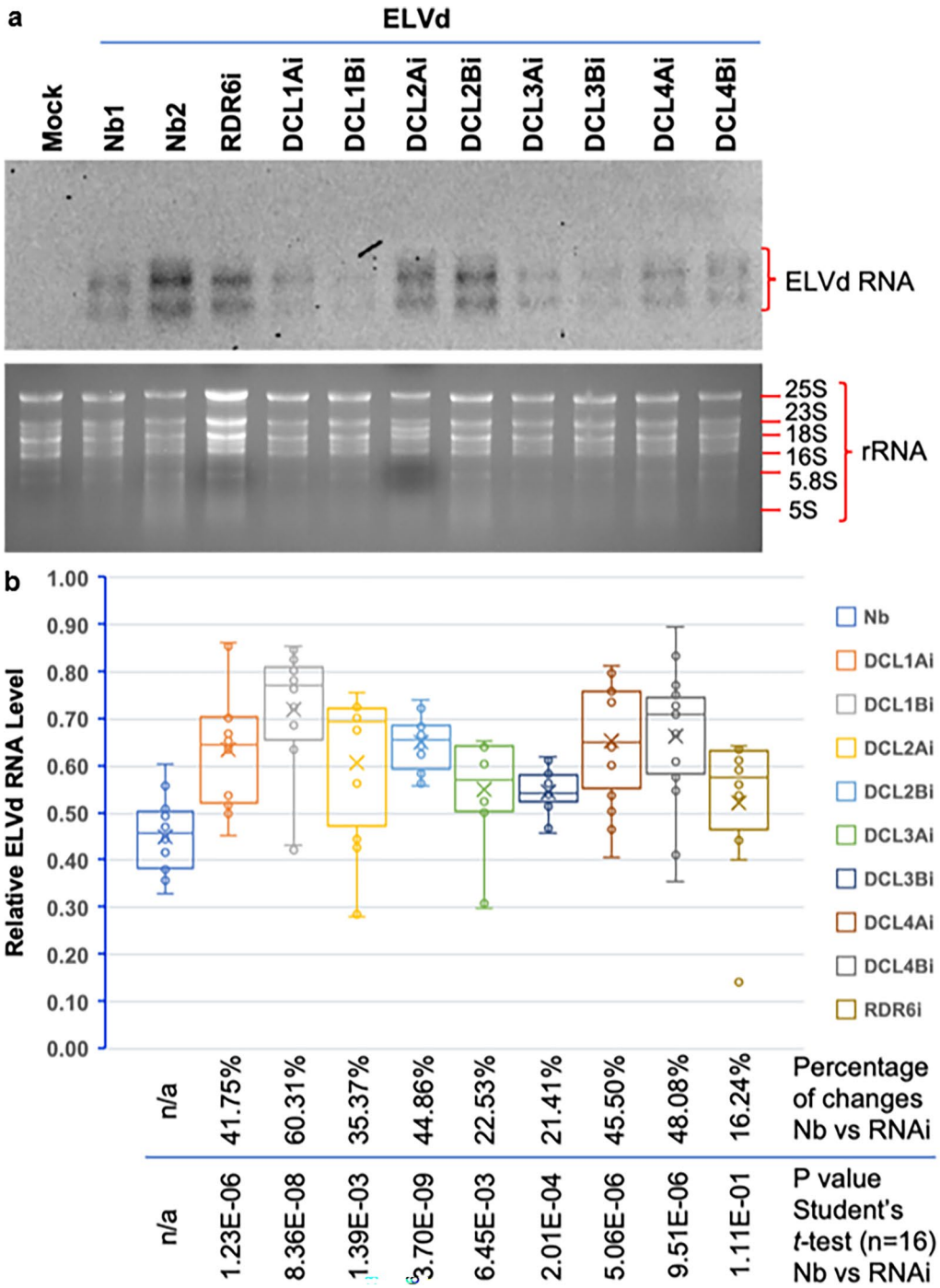

Fig. 1 Impact of *DCL*i and *RDR6i* on ELVd RNA accumulation at 6-dpi early infection. **a** Northern detection of ELVd RNA accumulation in wild-type *Nb*, *DCLi* and *RDR6i* plants. Total RNA extracted from mock *Nb* leaf tissues was included as a negative control. The blot was hybridized with ELVd-specific probe (upper panel). Ethidium bromide-stained gel shows loading of total RNA samples (lower panel). ELVd RNA and various sizes of rRNAs are indicated. **b** Quantitative analysis of ELVd RNA accumulation in wild-type *Nb*, *DCLi*, and *RDR6i* plants. Percentage of changes of ELVd RNA in *Nb* vs RNAi (*DCLi* and *RDR6i*), as well as *P* values of the Student's ***t***-test of ELVd RNA levels in *Nb* vs RNAi (*DCLi* and *RDR6i*) are indicated

similar trend of ELVd RNA level was found in *Nb* vs RNAi lines (Additional file 2: Figure S3a, b). Total sRNA profiles (Additional file 2: Figure S4a, b) and 21, 22, and 24 nt siRNAs that were mapped to individual RNA silencing pathway genes in these ELVd-infected *Nb* and transgenic plants (Additional file 1: Table S4)

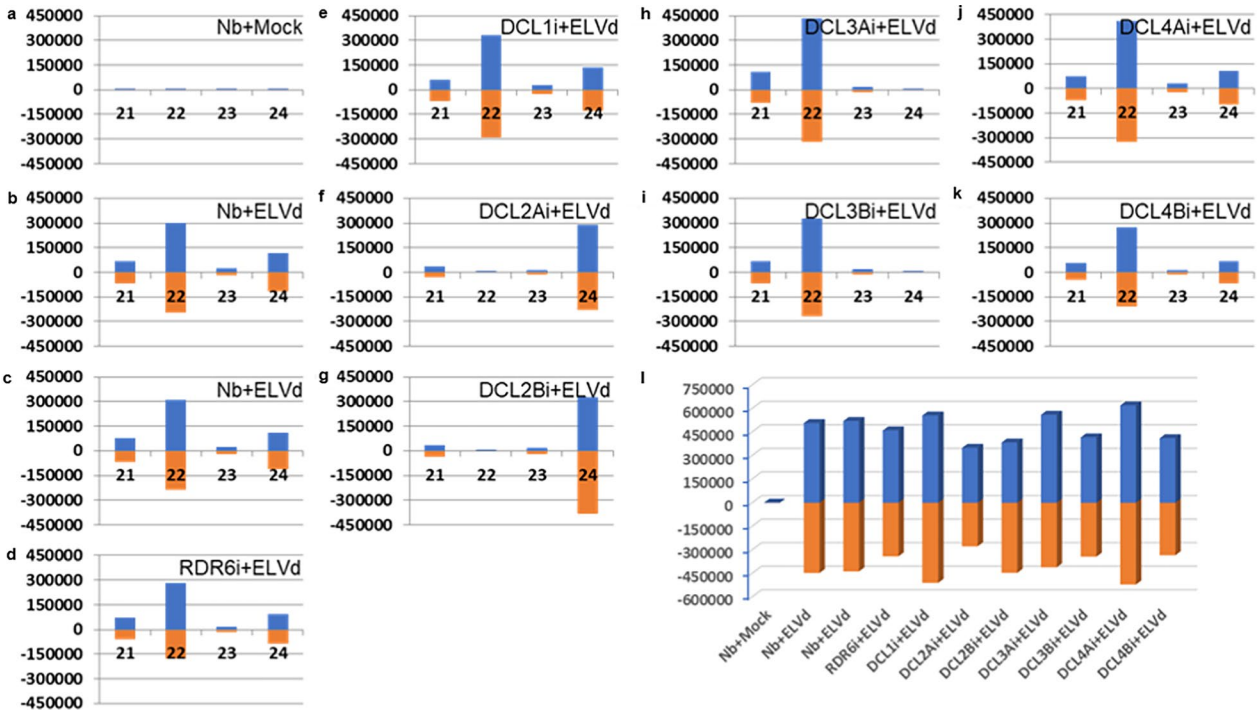

Fig. 2 Impact of *RDR6i* or *DCLi* on accumulation of ELVd 21–24 nt cvd-siRNAs at early stage of infection. **a** Mock inoculation of *N. benthamiana* (*Nb*). **b**, **c** *Nb* infected with ELVd. **d** *RDR6i* infected with ELVd. **e–k** *DCLi* infected with ELVd. *DCL1i* (**e**), *DCL2Ai* and *DCL2Bi* (**f** and **g**); *DCL3Ai* and *DCL3Bi* (**h** and **i**); *DCL4Ai* and *DCL4Bi* (**j** and **k**). **l** Total numbers of 21–24 nt cvd-siRNAs mapped to ELVd. Mock-inoculated or ELVd-infected leaf tissues were collected at 6 days post inoculation for sRNA analysis. Size profiles are shown for 21–24 nt cvd-siRNAs that were mapped to the ELVd RNA genome of both sense (blue) and complementary-sense (orange) strands

(See figure on next page.)

Fig. 3 Distribution of 21–24 nt cvd-siRNA at early stage of infection across the ELVd RNA genome. **a** Mock inoculation of *N. benthamiana* (*Nb*). **b**, **c** *Nb* infected with ELVd. **d** *RDR6i* infected with ELVd. **e–k** *DCLi* infected with ELVd. *DCL1i* (**e**), *DCL2Ai* and *DCL2Bi* (**f** and **g**); *DCL3Ai* and *DCL3Bi* (**h** and **i**); *DCL4Ai* and *DCL4Bi* (**j** and **k**). Mock-inoculated or ELVd-infected leaf tissues were collected at 6 days post inoculation for sRNA analysis. 21–24 nt cvd-siRNAs were mapped to the ELVd RNA genome of both sense and complementary-sense strands. Colour codes for each size of cvd-siRNAs and their polarities are indicated in each panel

were similar to those found in healthy controls (Additional file 1: Table S1; Additional file 2: Figure S1a, b). Size profiles for 21, 22, and 24 nt cvd-siRNAs and their distributions across the ELVd genome at 14 dpi in *Nb* or RNAi lines (Fig. 4a–l; Additional file 2: Figure S5a–k) were largely similar to those at 6 dpi (Fig. 2a–l, Fig. 3a–k). However, we noticed some changes of the total numbers of the 21, 22, and 24 nt cvd-siRNAs at the later stage of ELVd infection. Compared to *Nb* plants (Fig. 4b, c, and l), ELVd cvd-siRNAs reduced in *RDR6i* (Fig. 4d and l), whilst elevated in both *DCL3i* (Fig. 4h, i and l) and *DCL4i* plants (Fig. 4j–l) at 14 dpi.

Influence of ELVd infection on miRNA biogenesis

DCL1 is not particularly associated with generation of ELVd cvd-siRNAs. No miRNA-mediated anti-viroids has been reported. However cellular miRNAs produced by DCL1 are known to play an important role in plant defence against viruses and other pathogens (Simon-Mateo and Garcia 2006; Liu et al. 2017). We therefore analysed whether ELVd infection could affect cellular miRNA biogenesis (Fig. 5; Additional file 1: Tables S5, S6). At the early stage of infection, ELVd infection caused 64%–90% reduction of the total reads of 41 miRNA families in wild-type or *RDR6*- and *DCLs*-deficient plants, when compared with healthy wild-type *Nb* control (Fig. 5a; Additional file 1: Table S5). At the later

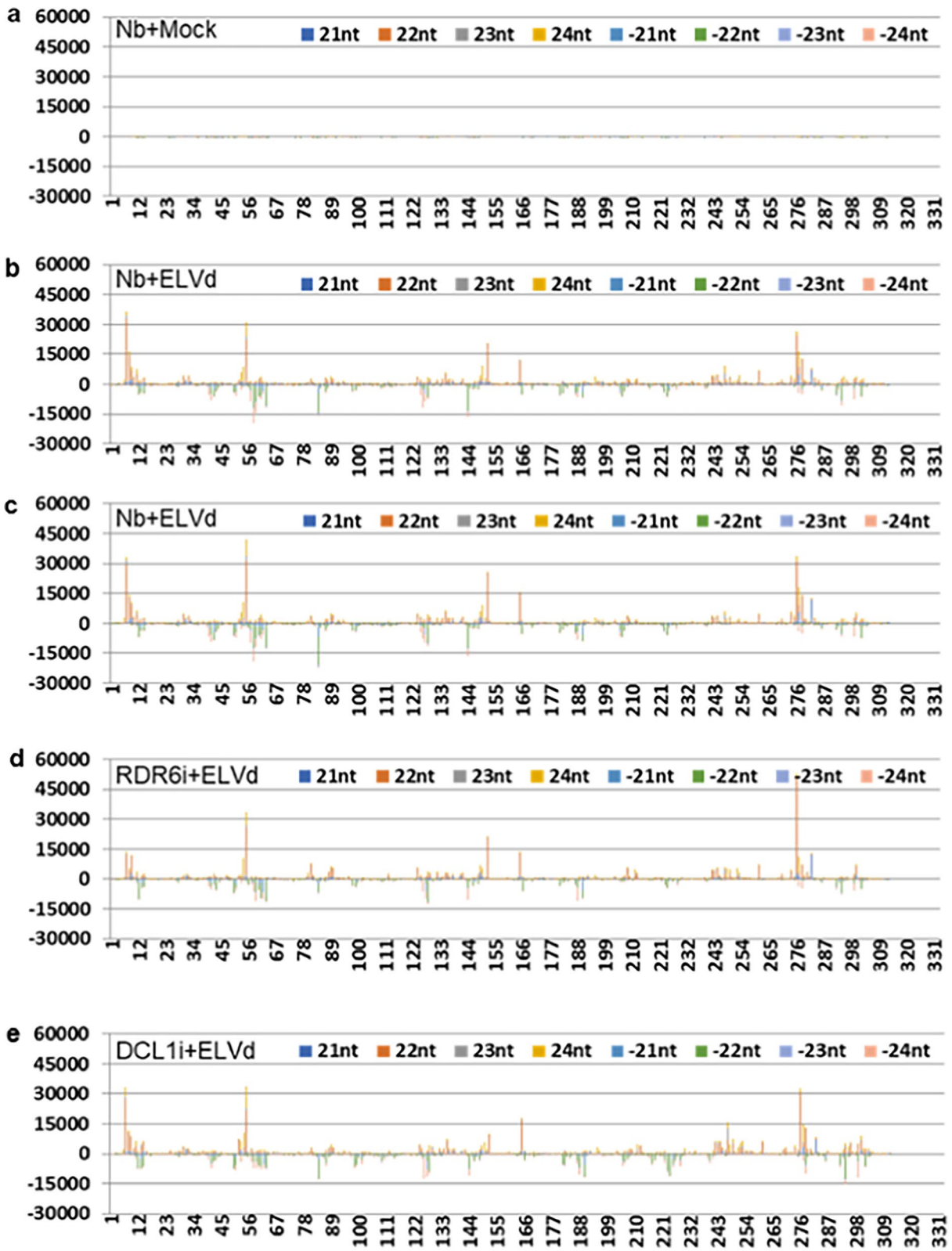

Fig. 3 (See legend on previous page.)

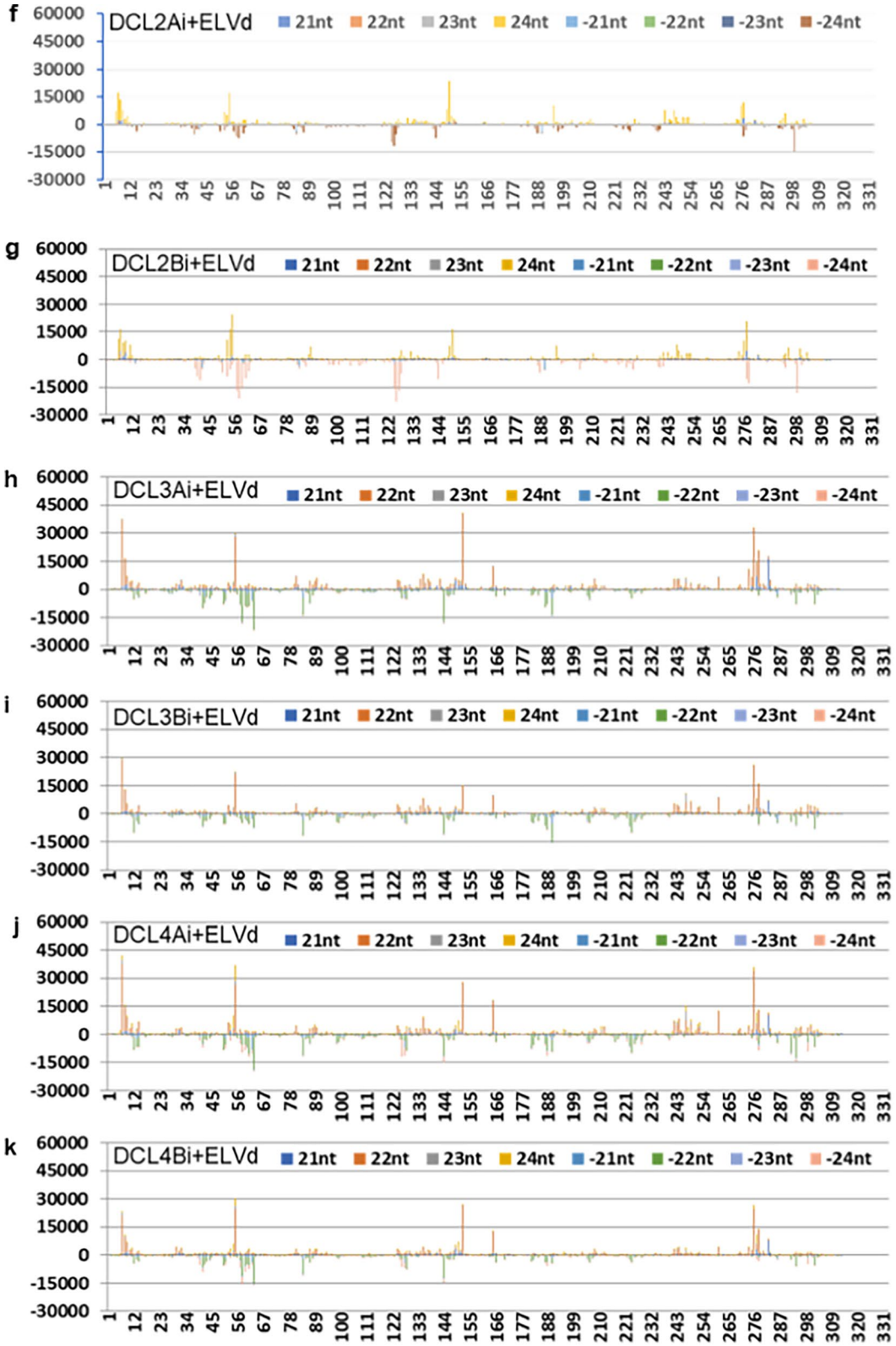

Fig. 3 continued

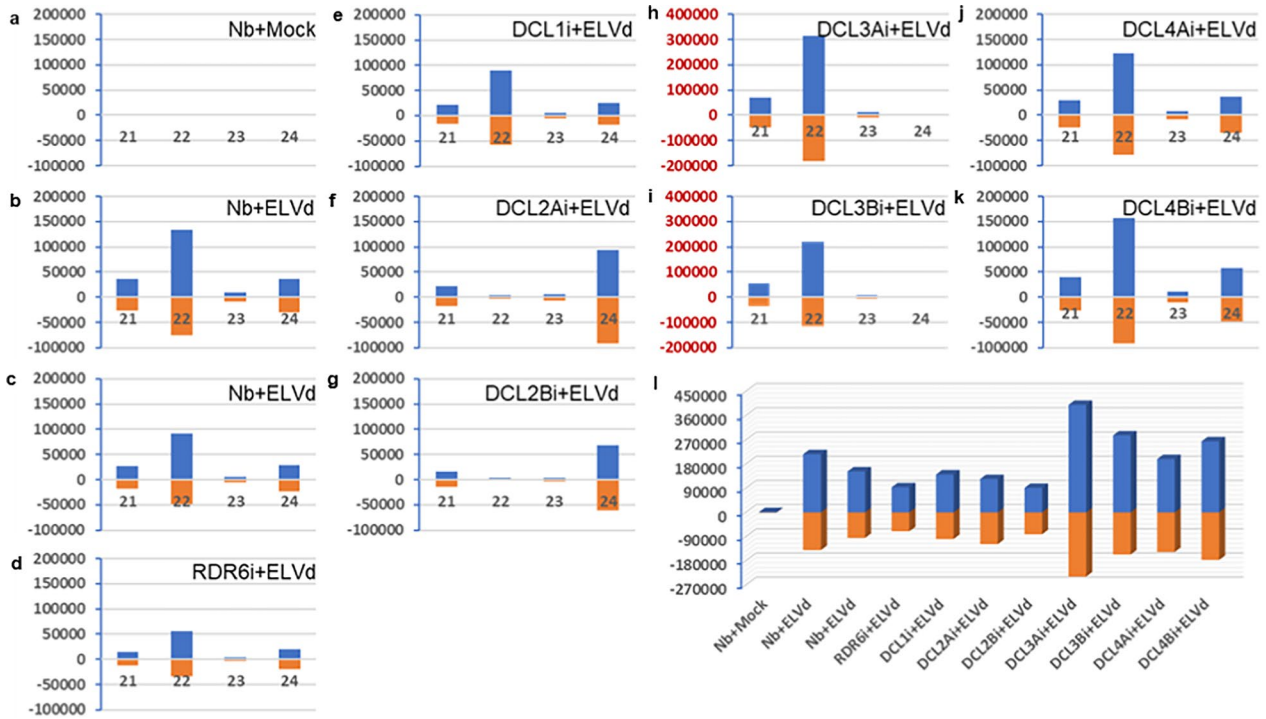

Fig. 4 Impact of *RDR6i* or *DCLi* on accumulation of ELVd 21–24 nt cvd-siRNAs at later stage of infection. **a** Mock inoculation of *N. benthamiana* (*Nb*). **b**, **c** *Nb* infected with ELVd. **d** *RDR6i* infected with ELVd. **e–k** *DCLi* infected with ELVd. *DCL1i* (**e**), *DCL2Ai* and *DCL2Bi* (**f** and **g**); *DCL3Ai* and *DCL3Bi* (**h** and **i**); *DCL4Ai* and *DCL4Bi* (**j** and **k**). **l** Total numbers of 21–24 nt cvd-siRNAs mapped to ELVd. Mock-inoculated or ELVd-infected leaf tissues were collected at 14 days post inoculation for sRNA analysis. Size profiles are shown for 21–24 nt cvd-siRNAs that were mapped to the ELVd RNA genome of both sense (blue) and complementary-sense (orange) strands

stage of infection, ELVd could still result in 21%–49% decrease of the total reads of 41 miRNA families in ELVd-infected *Nb*, *RDR6i*, and *DCLi* plants when compared with healthy wild-type *Nb* control (Fig. 5b; Additional file 1: Table S6).

Effect of ELVd infection on chloroplast-originating csRNA biogenesis

Avsunviroids reside and replicate inside chloroplasts. This prompted us to investigate whether ELVd infection would influence biological processes that may occur within chloroplasts, for instance, the impact of ELVd infection on csRNA production (Fig. 6). We first examined whether RNAs originated from chloroplast genome-encoding genes could be diced by DCLs in cytoplasm (i.e. outside chloroplasts). We constructed an RNAi vector to generate hairpin dsRNA (hp-dsRNA) for a 250-bp fragment corresponding to nucleotides 1181–1431 of the chloroplast *RbCL* gene (Fig. 6a). Such chloroplastic hp-dsRNAs, once expressed in *Nb* leaf tissues in the agroinfiltration assays (Fig. 6b), were readily targeted by cellular RNA silencing machinery for siRNA biogenesis (Fig. 6c, d). The siRNA size profiles were characteristic of the most abundant 21 nt siRNA along with a significant amount of 22 and 24 nt siRNAs, consistent with the patterns of siRNAs generated from nuclear (trans)gene mRNA and transient nuclear hp-dsRNAs (Chen et al. 2018). In the control *Nb* leaf tissues that were infiltrated with the empty RNAi vector, the size profile of csRNAs mapped to the 250-bp region of the *RbCL* mRNA was completely different from 21, 22, and 24 nt siRNAs generated from cellular RNA silencing, and the reads of csRNAs of various sizes from 20 to 28 nt were similar (Fig. 6e). Moreover, unlike nuclear gene mRNAs, no csRNA transitivity was observed, evidenced by the similar distribution of csRNAs along the other regions of the 2524-nt *RbCL* mRNA between hp-dsRNA expressing plants and no hp-dsRNA expressing controls (Fig. 7). Furthermore, the size profiles and total reads of csRNAs (Additional file 2: Figure S6) were similar among healthy wild-type *Nb*, *RDR6i*, *DCLi*, *DCL2i*, *DCL3i*, and *DCL4i* plants (Additional file 2: Figure S6a–j). However, compared to healthy controls (Additional file 2: Figures S6a, S7a), the total reads and individual reads of each size of 18–28 nt csRNAs (Additional file 2: Figure S7) reduced in wild-type *Nb*, *RDR6i*, *DCLi*, *DCL2i*, *DCL3i*, and *DCL4i* plants that were infected with ELVd (Additional file 2: Figure S7b–l). The size profiles of these reduced numbers

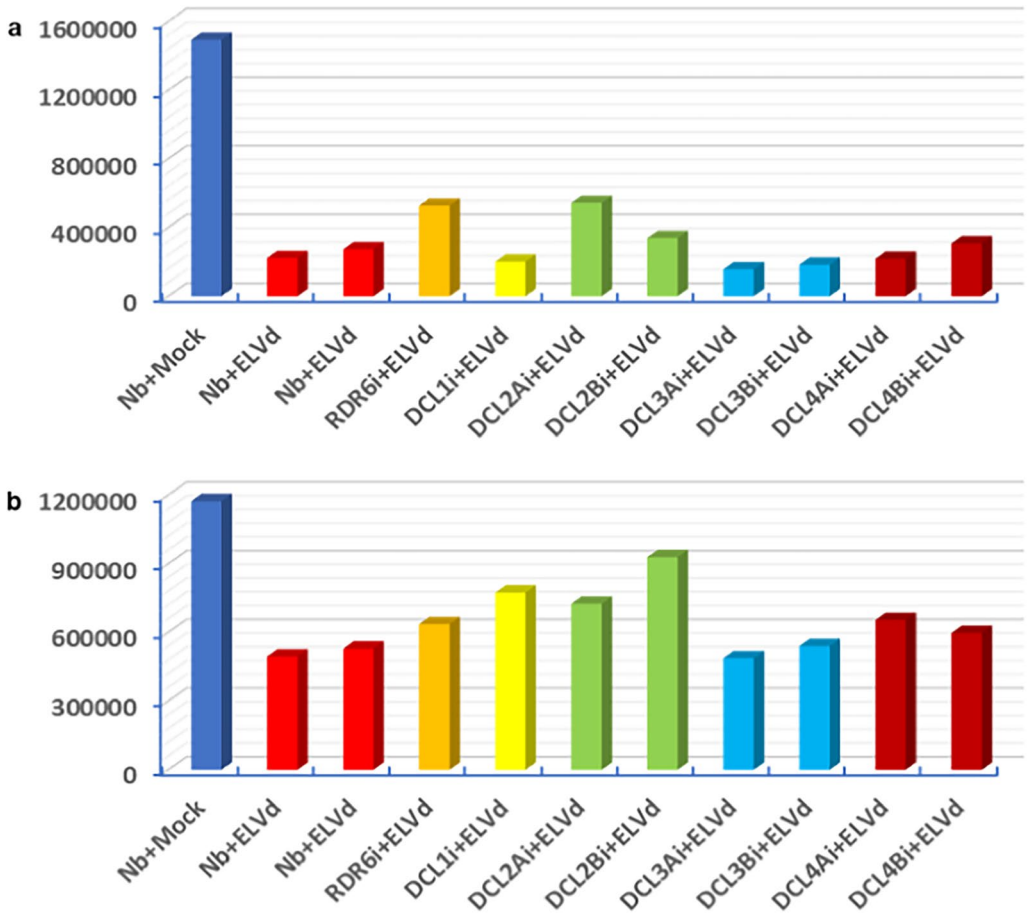

Fig. 5 Influence of ELVd on accumulation of cellular microRNAs at early and later stages of infection. **a** Early infection at 6 days post inoculation (dpi). **b** Later infection at 14 dpi. Mock-inoculated or ELVd-infected leaf tissues were collected at either 6- or 14-dpi for sRNA analysis. Mock inoculation of *N. benthamiana* (Nb + Mock), *Nb* infected with ELVd (Nb + ELVd), *RDR6i* infected with ELVd (RDR6i + ELVd) and *DCLi* infected with ELVd (*DCL1i* + ELVd, *DCL2Ai* + ELVd, *DCL2Bi* + ELVd, *DCL3Ai* + ELVd, *DCL3Bi* + ELVd, *DCL4Ai* + ELVd, *DCL4Bi* + ELVd) are indicated

of csRNAs were similar among all ELVd-infected *Nb* and *RNAi* plants at 6 dpi (Additional file 2: Figure S7b–l). Such suppression of csRNA accumulation endured to the later stage of ELVd infection at 14 dpi (Additional file 2: Figure S8).

Discussion

In this article, we report how plant responds to infection by a chloroplastic viroid by examining impacts of RNA silencing on ELVd cvd-siRNA biogenesis. Our work extends the understanding of plant anti-viroid mechanism in the following aspects.

1. In *DCL1i*, *DCL2i*, *DCL3i*, and *DCL4i* plants ELVd RNA level increased at early and later stage of infection (Fig. 1; Additional file 2: Figure S3). However, *RDR6* impacts less on ELVd RNA accumulation. This suggests that four *DCLs* may all be involved in plant defense against ELVd infection.
2. The profile for ELVd 21, 22, and 24 nt cvd-siRNAs (Figs. 2, 3) differs from that of nucleus-replicating viroids (Martin et al. 2007; Martinez et al. 2010; Jiang et al. 2019), plant RNA (Qin et al. 2017) and DNA (Blevins et al. 2006) viruses, transgene mRNA and hairpin dsRNA (Chen et al. 2018), and indeed other chloroplast-replicating viroids such as peach latent mosaic viroid (PLMVd, Di Serio et al. 2009; St-Pierre et al. 2009). Such comprehensive cvd-siRNA profile might be verified by sRNA Northern blotting. Nevertheless, our sRNAseq results indicate that DCL2 was essential to produce the most abundant 22 nt cvd-siRNAs (Figs. 2, 4). When *DCL2* was knocked down in the two *DCL2*-RNAi lines, ELVd was then predominantly targeted by *DCL3* for generating 24 nt cvd-siRNAs (Figs. 2, 4). These data suggest that *DCL2* acts primarily in anti-ELVd RNA silencing whilst *DCL3* is redundant to *DCL2*. This differs from the synergistic and combined activity of *DCL2* and

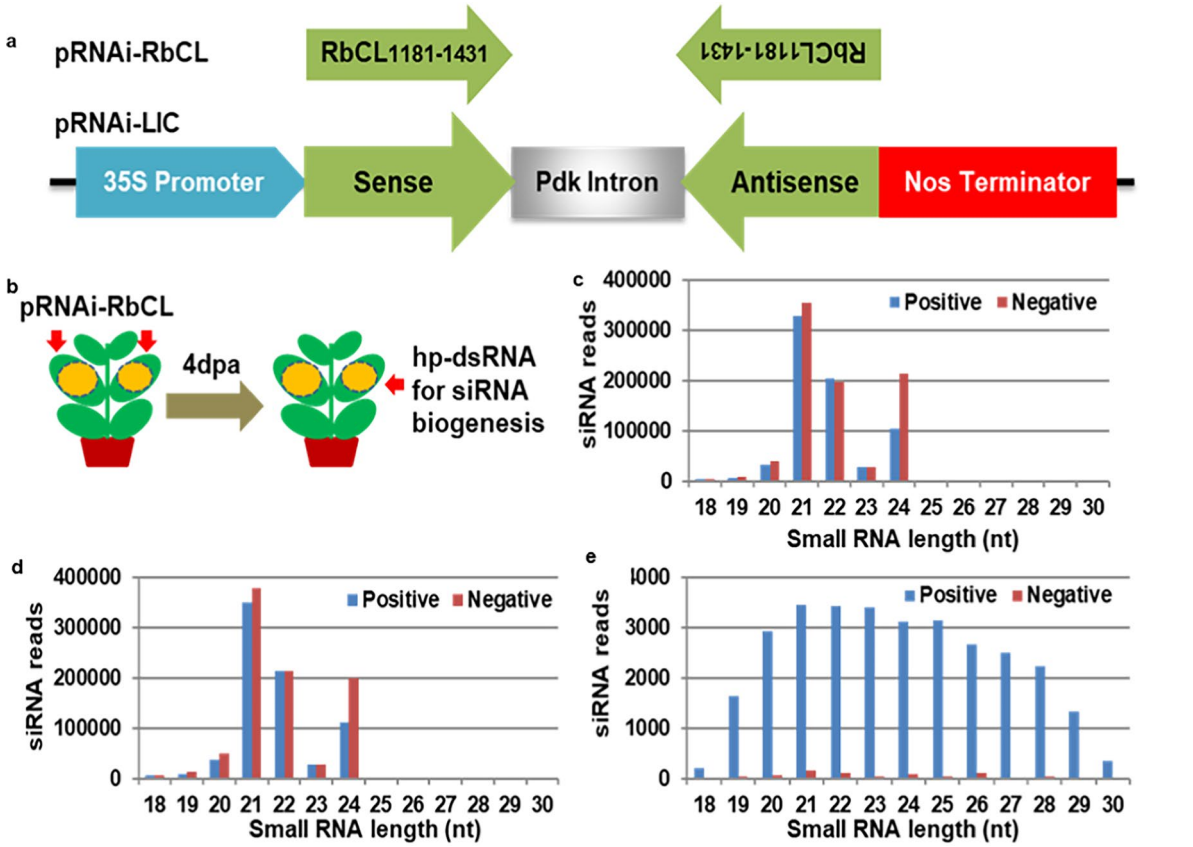

Fig. 6 Production of chloroplast gene sRNA in cytoplasm. **a** Diagrammatic of pRNAi-RbCL construct. **a** 250-bp fragment corresponding to the nucleotide region 1181–1431 was inverted cloned into the pRNAi-LIC vector in order to generate hp-dsRNA for siRNA biogenesis in plant cell cytoplasm. **b** Experimental design. Leaves of *N. benthamiana* plant at the six-leaf stage were infiltrated with agrobacterium carrying either the empty pRNAi-LIC vector or pRNAi-RbCL. At 4-days post agroinfiltration, leaf tissues were collected, pooled and used for sRNA analysis. **c–e** Profiles of 18–30 nt siRNAs mapped to the 250 nt portion of the *RbCL* mRNA. Leaf tissues expressed *RbCL* hp-dsRNA (**c** and **d**) and controls expressed no *RbCL* hp-dsRNA (**e**). Specific siRNAs were mapped to both mRNA (positive) and complementary (negative) strands of the *RbCL* mRNA fragment (nucleotides 1181–1431)

DCL3 in silencing-based defence against nucleus-replicating viroids such as PSTVd (Dalakouras et al. 2015; Katsarou et al. 2016).

3. *DCL4* is required for efficient nucleus-replicating viroid infection, leading to increase in vd-siRNAs in plants (Dalakouras et al. 2015; Katsarou et al. 2016). However, *DCL4* had little effect on accumulation of ELVd cvd-siRNA at the early stage of infection and the DCL4-processed 21 nt cvd-siRNA was least abundant in infected plants (Figs. 2, 4). At the later infection stage (i.e., 14 dpi), deficiency in *DCL4* (and *DCL3*) allow escalating levels of ELVd, which would then be targeted by RNA silencing machinery to generate more abundant cvd-siRNAs (Fig. 4). Such temporal differences in cvd-siRNA accumulation may reflect a dynamic RNA silencing-mediated defence during the course of ELVd infection, and/or an active escaping strategy for ELVd to survive such cellular defence since ELVd (and all other viroids) encodes no suppressors of silencing (van Wezel and Hong 2004).
4. *DCL1* is not directly involved in biogenesis of ELVd cvd-siRNAs (Figs. 2, 4). However, ELVd infection suppresses plant miRNA accumulation independent of *RDR6* and *DCLs* (Fig. 5). These results suggest that miRNAs might indirectly contribute to plant cellular anti-ELVd defence, for instance, via regulation of plant immunity genes by miRNAs. On the other hand, host cells can alleviate ELVd-mediated suppression of miRNA biogenesis to adapt to ELVd at the later stage of infection (Fig. 5). Furthermore, considering the reduction of cvd-siRNAs in *RDR6i* plants at 14 dpi (Fig. 4), any possible involvement of *RDR6* in combating later ELVd infection might be also indirect. Further detection and quantitation of cvd-siRNAs by sRNA Northern blotting may clarify

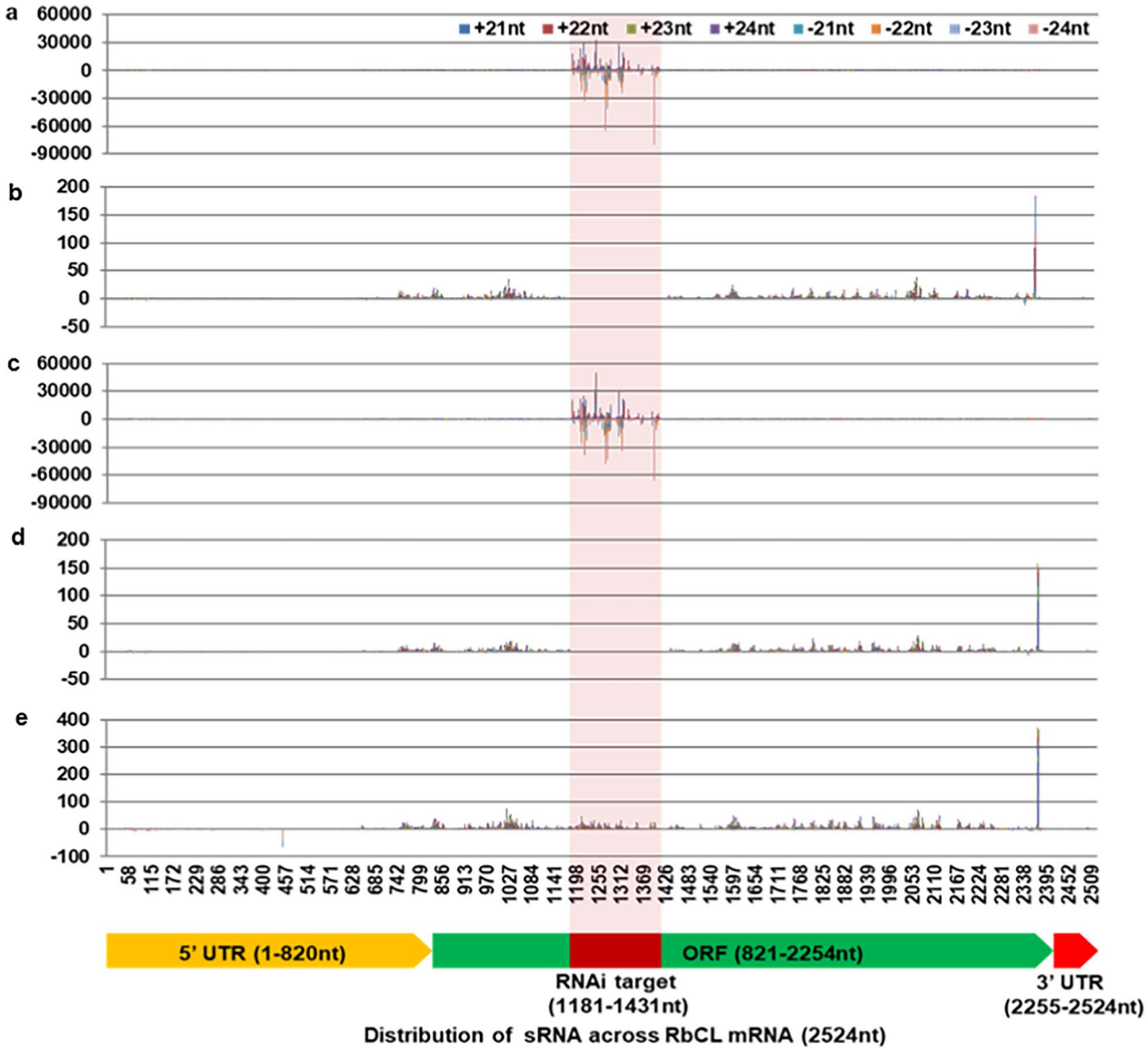

Fig. 7 No silencing transitivity in generation of chloroplastic small RNAs. **a** to **d** Distribution of 21–24 nt chloroplastic small RNAs (csRNAs) across the entire *RbCL* transcript. In *N. benthamiana* leaf tissues expressing the *RbCL* hp-dsRNA (**a** and **c**), abundant 21–24 nt siRNAs generated in cytoplasm were mapped to the RNAi targeted region (nucleotides 1181–1431). However, only very low levels of 21–24 nt csRNAs were found to be mapped to the 5′- and 3′-UTRs or non-targeted region of the *RbCL* mRNA (**b** and **d**). It should be noted that the reads of specific csRNAs mapped to the RNAi target region were left out in order to show the low levels of csRNAs across the rest *RbCL* mRNA portions. **e** Distribution of background 21–24 nt csRNAs across the *RbCL* mRNA in control plants expressing no *RbCL* hp-dsRNA. Specific siRNAs were mapped to both mRNA (positive) and complementary (negative) strands of *RbCL* mRNA (nucleotides 1–2524). Colour codes for each size of csRNAs and their polarities are indicated

the precise role of RDR6 in dynamic cvd-siRNA biosynthesis during ELVd infection.

5. Chloroplastic mRNA, if transcribed in nucleus and presented in cytoplasm, can be targeted by cytoplasmic DCLs-based RNA silencing for biogenesis of 21, 22, and 24 nt siRNAs (Figs. 6, 7). However, chloroplastic mRNA, if expressed within chloroplasts, cannot be diced by cellular DCLs. Our findings thus imply that csRNA may be produced by a chloroplast-specific sRNA-processing machinery. This is consistent with the distinct csRNA size profiles (Fig. 6), no csRNA transitivity for the chloroplast *RbCL* mRNA (Fig. 7), and reduction of csRNAs in ELVd-infected *Nb*, *RDR6i* and *DCLi* plants (Additional file 2: Figures S6, S7). The precise nature of such chloroplast-specific sRNA-processing machinery is presently

unknown. Furthermore, any role of csRNAs in ELVd-plant interaction or/and in regulation of chloroplastic genes also remains to be elucidated.

6. Viroids in the family *Avsunviroidae* replicate and accumulate in chloroplasts (Bonfiglioli et al. 1994; Navarro et al. 1999; Daròs 2016). However, particularly in the case of ELVd, a nuclear stage during life cycle was also showed (Gómez and Pallás 2012). Such chloroplastic and nuclear subcellular compartmentalization should prevent ELVd from attack by RNA silencing which operates mainly in cytoplasm (Fig. 8). The difference between the size profiles of RNA silencing-originated siRNAs and *bona fide* csRNAs also indicate that any key components of the cellular RNA silencing machinery such as DCL2 are not imported into chloroplasts. To explain these results, we envisage that a cytoplasm phase may exist during ELVd trafficking between nucleus and chloroplasts within infected cells and during the cell-to-cell and long-distance movement through the infected plant (Fig. 8). When ELVd enters cytoplasm at the early infection, cytoplasmic RNA silencing can immediately target and process ELVd genomic RNA into 21, 22, and 24 nt siRNAs. At a later stage, cytoplasmic ELVd-derived RNAs may require cellular RDR6 to produce dsRNA for further cleavage into siRNAs (Fig. 8). This model provides a plausible link between and logically reconciles the two seemingly contradictory aspects of cytoplasmic RNA silencing versus cvd-siRNA production together in plants.

Conclusions and future outlook

In summary, through sRNA profiling of the ELVd cvd-siRNAs and csRNAs in *Nb*, *RNA6i*, and *DCLi* plants, we reveal that *DCL2* plays an essential role in RNA silencing-mediated defence against chloroplast-replicating ELVd. *DCL3* is functionally redundant to *DCL2* in terms of targeting ELVd RNA for cvd-siRNA biogenesis. The roles of *DCL4* are complex and dynamic in anti-ELVd. No direct involvement of *DCL1* in cellular defence against ELVd was observed, but DCL1-processed miRNAs may indirectly participate in protection of plants from ELVd attack. Our results also demonstrate that sRNAs derived

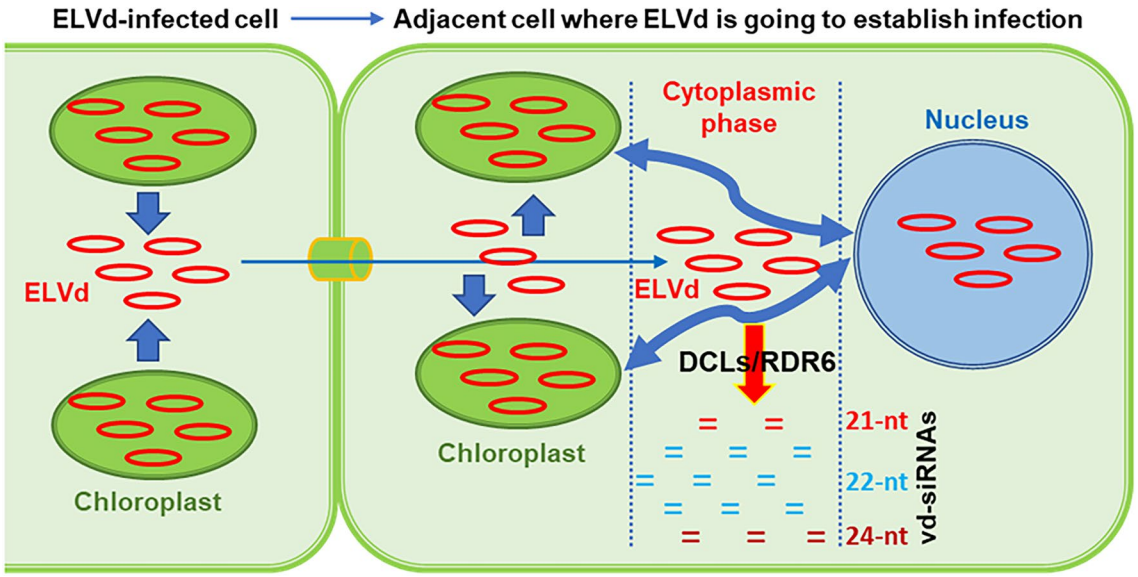

Fig. 8 A working model for cvd-siRNA biogenesis for chloroplast-replicating viroids. ELVd, a chloroplastic viroid, replicates in chloroplasts and it also endures a nuclear stage during its infection cycle. Such distinct subcellular compartments should prevent cytoplasmic RNA silencing machinery from targeting and cleaving ELVd RNA to generate cvd-siRNAs. However, siRNAs that are processed by RNA silencing and *bona fide* csRNAs are different, suggesting that ELVd cvd-siRNAs are not produced in chloroplasts. We envisage that a cytoplasmic phase during the shuttling of ELVd between cells via plasmodesmata (represented by a cylinder) or from chloroplast to nucleus and vice versa (blue double-arrow line) within infected cells may exist. Thus, when ELVd enters cytoplasm *en route* from chloroplast to nucleus *or* intercellular movement via plasmodesmata, for example, at the early stage of infection, cytoplasmic RNA silencing machinery can immediately target and process ELVd genomic RNA into cvd-siRNAs by DCLs. DCL2 is the predominant DCL to cleave ELVd RNA for production of 22 nt cvd-siRNA. DCL3 is functionally redundant to DCL2. Only when DCL2 is deficient, DCL3 dices ELVd RNA into 24 nt cvd-siRNA. DCL1, DCL4, and RDR6 may not be directly involved in such defence at the early stage of ELVd infection. However, at a later stage, they may be also required. For example, RDR6 may act to convert ELVd ssRNA into dsRNA for further cleavage into siRNAs in cytoplasm. This working model provides a plausible link between and logically reconciles the two seemingly contradictory aspects of cytoplasmic RNA silencing versus cvd-siRNA production together. ELVd circular ssRNA, chloroplasts, nucleus and ELVd-siRNAs of various sizes are indicated

from nuclear and chloroplast genes may involve different silencing machineries. The dynamic changes of csRNAs during ELVd infection suggests that csRNAs may be of biological relevance to interactions between chloroplastic viroids and their host plants. Moreover, this research has opened new frontiers for further investigation. For instance, how does the cellular RNA silencing recognize chloroplast-replicating viroids to eliminate their infection? Can cvd-siRNAs or siRNAs in general act as intracellular signals to trigger spread of RNA silencing between cytoplasm and chloroplast and vice versa within cells? What is the genetic and molecular basis for csRNA biosynthesis in chloroplast? Can csRNA function as retrograde-signalling molecules to regulate nuclear gene expression? What is the potential application of cvd-siRNAs in plant genetic engineering or even as exogenous sRNA agents (Mohamed et al. 2022) for viroid resistance? Answers to these questions will advance our understanding of chloroplastic RNA silencing mechanisms in plants.

Methods

Plant materials and growth conditions

Generation of transgenic RNAi *N. benthamiana* (*Nb*) lines including *RDR6i*, *DCL1Ai*, *DCL1Bi*, *DCL2Ai*, *DCL2Bi*, *DCL3Ai*, *DCL3Bi*, *DCL4Ai*, and *DCL4Bi* was previously described (Chen et al. 2018). Briefly, pRNAi-RDR6i and pRNAi-DCLi were constructed in the pRNAi-LIC vector. These RNAi constructs were then mobilized into *Agrobacterium tumefaciens* strain LBA4404. *Agrobacterium*-mediated transformation was performed on *Nb* leaf discs to generate primary transgenic plants. Homozygous lines with a single copy of each RNAi construct were obtained from primary transformants after selfing and genetic analyses (Chen et al. 2018). Wild-type *Nb* and all transgenic plants were grown and maintained in insect-free glasshouses or growth-rooms at 25°C with supplementary light (13,000 Lux intensity/Visible 40W LED Light Bulbs) to give a 16-h photoperiod.

Eggplant latent viroid infection

The original ELVd infectious clone p53ELVd (GenBank reference sequence NC_039241.1), previously constructed in José-Antonio Daròs laboratory (Additional file 2: Figure S9), was subcloned into pCAMBIA1300 (Yu et al. 2018) to produce p1300/35S-ELVd. This was achieved by PCR amplification of a fragment covering the entire ELVd cassette (Additional file 2: Figure S9a) by a pair of primers 1300-35S-ELVd F/KpnI (5' aaaaaa*GGTACC*GATTCCATTGCCCAGCTATC 3') and 1300-35S-ELVd R/PstI (5' aaaaaaCTGCAGCTG GATTTTGGTTTTAGGAA 3'), and cloning the resultant PCR product into the *Kpn*I/*Pst*I sites of pCAMBIA1300 (Additional file 2: Figure S9b). Recombinant clones were screened by PCR using a pair of primers 1300-seq-F (5' CGCAATTAATGTGAGTTAGCTCAC 3') and 1300-seq-R (5' ATCGGTGCGGGCCTCTTCGC 3'). Miniprep plasmid DNA was doubly digested with *Kpn*I/*Pst*I to confirm the right insert (Additional file 2: Figure S9c) and further verified by Sanger sequencing. Plasmid p1300/35S-ELVd was then transformed into *Agrobacterium tumefacien* GV3101. Agrobacterium carrying p1300/35S-ELVd was cultured, collected and resuspended in sterile water at optical density at 600 nm (OD_{600}) of 1.0. Young leaves of *Nb* and transgenic RNAi plants at the stage of 6 leaves were agro-infected as previously described (Bruce et al. 2011).

Induction of RNA silencing against chloroplast mRNA and agroinfiltration

To investigate if cytoplasmic RNA silencing targets chloroplast gene-encoded mRNA, we generated a gene-specific hairpin *RbCL*-RNAi vector pRNAi-RbCL (Fig. 6a) that targets the *chlororibulose-1, 5-bisphosphate carboxylase/oxygenase large subunit* (*RbCL*) gene (Additional file 2: Figure S10; Shinozaki and Sugiura 1982; Kunnimalaiyaan and Nielsen 1997). To make this construct, cDNA fragments (250 bp) corresponding to nucleotides 1182 to 1431 of *RbCL* (GenBank no. J01450.1; Additional file 2: Figure S10) was amplified using a set of primers NbRbCL RNAi-F (5' CGACGACAAGACCCTtaggtaacgtatttgggttca 3') and NbRbCL RNAi-R (5' GAGGAGAAG AGCCCTtcatcatctttagtaaaatca 3') and cloned into the RNAi vector pRNAi-LIC as described (Xu et al. 2010). Two young leaves per *Nb* plant (six plants at the six-leaf stage in each experiment) were infiltrated with 1 OD_{600} *A. tumefaciens* GV3101 harbouring pRNAi-RbCL or the empty RNAi vector. Agro-infiltrated leaf tissues from three to four different plants at 4 days post agroinfiltration, were collected and pooled together. Two pooled samples from different plants were used for sRNA extraction and construction of sRNA libraries.

RNA extraction, Northern blot, and RT-PCR

Total RNA was extracted from agroinfiltrated leaf tissues using RNAprep Pure Plant Kit (Tiengen). Northern blot was performed as previously described to detect ELVd RNA using an ELVd-specific probe (van Wezel and Hong 2004; Chen et al. 2018). Briefly, 5 μg of RNAs extracted from leaf tissues were separated on a 1% formaldehyde agarose gel, transferred to Hybond-N + membranes (Amersham Biosciences) through upward capillary transfer in 20 × SSC buffer, then crosslinked to the membrane with an UVP CX 2000 UV crosslinker at 120 mJ/cm^2 for 1 min. Membranes were hybridized with digoxigenin-labeled ELVd-specific probe that were prepared using the DIG High Prime DNA Labeling Kit (Roche).

Hybridization was detected using a DIG Nucleic Acid Detection Kit (Roche) as recommended by the manufacturer. Chemilluminescent signals were detected with a ChemiDoc XRS + imaging System (Bio-Rad). Furthermore, RT-PCR was performed to quantify ELVd RNA accumulation. Briefly, cDNA was reverse-transcribed from 1 μg total RNA pre-treated in with gDNase using Fastking RT Kit (With gDNase; Tiengen) in 20 μL solution containing 2 μL 10 × King RT Buffer, 2 μL FQ-RT Primer Mix, and 1 μL Fastking RT Enzyme Mix. PCR was then carried out in 20 μl solution containing the ELVd-specific primers ELVd-3F/ELVd-3R (Additional file 2: Figure S9a), 1 μL cDNA, 2 × Taq Master Mix (CWBIO) at 95°C for 5 min, followed by 35 cycles of 95°C for 30 s, 58°C for 30 s and 72°C for 30 s; and then at 72°C for 10 min. PCR detection of 18S rRNA with Primers PP271F (5' CGGCTACCACATCCAAGGAAGG 3')/ PP272R (5' GAGCTGGAATTACCGCGGCTG 3') was used as a control of adding equal amount of cDNA in all PCRs. After electrophoresis of 10 μL PCR product in 1.0% agarose gel and stained in ethidium bromide, the relative intensity of ELVd specific bands was quantified by ImageJ software, and analysed by the Student's ***t***-test.

Construction of small RNA Library for small RNA sequencing

Low-molecular-mass sRNAs were enriched from total RNA as described (Hamilton and Baulcombe 1999). Fragments of 18–30 nt long RNA were isolated from total RNA extracted from pooled samples of three to four different plants for each of the biological and technical duplicates after being separated through 15% denaturing polyacrylamide gel/7 M urea gel electrophoresis in 1 × Tris–borate-EDTA buffer. Then, sRNAs were excised from the gel and sequentially ligated to a 39-nt adapter and a 59-nt adapter. After each ligation step, sRNAs were purified after 15% denaturing PAG/7 M urea electrophoresis. The final purified ligation products were reverse-transcribed into cDNA using reverse transcriptase (Finnzymes Oy). The first strand cDNA was PCR amplified using the high-fidelity Phusion* DNA Polymerase (Finnzymes Oy). The purified DNA fragments were used for clustering and sequencing by Illumina HisEquation 2000 (Illumina) at the Beijing Genomics Institute.

Bioinformatics analysis of small RNA sequences

Illumina HighSEquation 2000 sequencing produced a similar number of 28 million reads per sRNA library. The reads were cropped to remove adapter sequences and were aligned to the reference sequences using Bowtie2 (Langmead and Salzberg 2012). Reference sequences include ELVd RNA genome (GenBank number NC_039241.1, same as AJ536613.1; Additional file 2: Figure S9a; Fadda et al. 2003), *RbCL* (GenBank number J01450.1; Additional file 2: Figure S10; Shinozaki and Sugiura 1982; Kunnimalaiyaan and Nielsen 1997), *DCL1* (GenBank number FM986780), *DCL2* (GenBank number FM986781), *DCL3* (GenBank number FM986782), *DCL4* (GenBank number FM986783) and other RNA silencing pathway gene sequences (Nakasugi et al. 2013; Chen et al. 2018) and a set of 41 unique tobacco miRNA sequences identified in *Nicotiana* plants (Pandey et al. 2008; Nakasugi et al. 2014). SAMtools pileup was used to produce the siRNA and miRNA coverage profiles (Li et al. 2009). Outcomes of comparisons between normalized cvd-siRNA, microRNA or csRNA reads against the total sRNA reads (per 10 million sRNA reads) are consistent with the numbers of cvd-siRNA, microRNA, or csRNA reads directly compared.

Abbreviations

AGO	Agronaute
ASBVd	*Avocado sunblotch viroid*
csRNA	Chloroplastic small RNA
cvd-siRNA	Chloroplastic viroid siRNA
DCL	DICER-LIKE endonuclease
ELVd	*Eggplant latent viroid*
PSTVd	*Potato spindle tube viroid*
RbCL	*Chlororibulose-1, 5-bisphosphate carboxylase/oxygenase large subunit*
RDR	RNA-dependent RNA polymerase
siRNA	Small interfering RNA
vsiRNA	Viral siRNAs

Supplementary Information

The online version contains supplementary material available at https://doi.org/10.1186/s42483-025-00351-3.

Additional file 1: Table S1. 21–24 nt sRNAs mapped to RNAi pathway genes in healthy plants. **Table S2.** Impact of *DCLi* and *RDR6i* on microRNA biosynthesis in healthy plants. **Table S3.** Impact of ELVd early infection on 21–24 nt sRNAs mapped to RNAi pathway genes. **Table S4.** Impact of ELVd later infection on 21–24 nt sRNAs mapped to RNAi pathway genes. **Table S5.** Impact of ELVd early infection on microRNA biogenesis. **Table S6.** Impact of ELVd later infection on microRNA biogenesis.

Additional file 2: Figure S1. Total small RNA/microRNA reads from healthy control plants. **Figure S2.** Impact of ELVd early infection on cellular small RNA accumulation. **Figure S3.** Impact of *DCLi* and *RDR6i* on ELVd RNA accumulation at 14-dpi later infection. **Figure S4.** Impact of ELVd later infection on cellular small RNA accumulation. **Figure S5.** Distribution of 21–24 nt cvd-siRNA associated with later infection across ELVd genome. **Figure S6.** Reduction of chloroplast csRNAs by ELVd later infection. **Figure S7.** ELVd reduces accumulation of chloroplastic small RNAs at early infection stage. **Figure S8.** Reduction of chloroplast csRNAs by ELVd at the later stage of infection. **Figure S9.** Construction of ELVd infectious clone. **Figure S10.** Sequence of the chloroplast gene *RbCL* mRNA.

Acknowledgements

We are grateful to Cheng Qin, Zhiming Yu, Nongnong Shi, Chengyong He, Zhixiang Zhang, Qianqian Chen, Yicheng Jin, and Zhen Liu for their inputs and technical support, and to Ping Ma for his advice on bioinformatics analysis for this work. We would like to dedicate this paper to our colleague, Dr. Toba Osman. Sadly, he passed away during the preparation of this paper for publication.

Author contributions
PZ designed and performed experiments and analyzed data; XZ performed bioinformatics analysis; AMM and LW performed research; JAD, SL, and MT were involved in the analysis of data and helped writing the article; YH conceived and initiated the project, designed experiments, analyzed data, and wrote the article.

Funding
This work was in part supported by grants from the Hangzhou Joint Fund of the Zhejiang Provincial Natural Science Foundation of China (LHZY24C140001), the Ministry of Science & Technology of China (Key International R&D Program 2017YFE0110900), the National Natural Science Foundation of China (31872636), the Ministry of Agriculture of the People's Republic of China (National Transgenic Program of China 2016ZX08009001-004), Hangzhou Normal University (Sino-EU Plant RNA Signaling S&T Platform Initiative 2018PYPTL001), Chinese Academy of Tropical Agricultural Sciences (Central Public Interest Scientific Institution Basal Research Fund for Chinese 1630042019017), and the Spanish Ministerio de Ciencia e Innovación (BIO2017-83184-R; co-financed European Union FEDER funds).

Availability of data and materials
Not applicable.

Declarations

Ethics approval and consent to participate
Not applicable.

Consent for publication
Not applicable.

Competing interests
The authors declare that they have no competing interests.

Received: 25 November 2024 Accepted: 17 April 2025
Published online: 24 July 2025

References

Adkar-Purushothama CR, Perreault JP. Current overview on viroid–host interactions. Wires RNA. 2020;11(2): e1570. https://doi.org/10.1002/wrna.1570.
Aliyari R, Ding SW. RNA-based viral immunity initiated by the Dicer family of host immune receptors. Immunol Rev. 2009;227(1):176–88. https://doi.org/10.1111/j.1600-065X.2008.00722.x.
Aregger M, Borah BK, Seguin J, Rajeswaran R, Gubaeva EG, Zvereva AS, et al. Primary and secondary siRNAs in Geminivirus-induced gene silencing. PLoS Pathog. 2012;8(9): e1002941. https://doi.org/10.1371/journal.ppat.1002941.
Bonfiglioli RG, McFadden GI, Symons RH. *In situ* hybridization localizes avocado sunblotch viroid on chloroplast thylakoid membranes and coconut cadang cadang viroid in the nucleus. Plant J. 1994;6(1):99–103. https://doi.org/10.1046/j.1365-313X.1994.6010099.x.
Baulcombe D. RNA silencing in plants. Nature. 2004;431(7006):356–63. https://doi.org/10.1038/nature02874.
Bolduc F, Hoareau C, St-Pierre P, Perreault JP. In-depth sequencing of the siRNAs associated with peach latent mosaic viroid infection. BMC Mol Biol. 2010;11:16. https://doi.org/10.1186/1471-2199-11-16.
Blevins T, Rajeswaran R, Shivaprasad PV, Beknazariants D, Si-Ammour A, Park HS, et al. Four plant Dicers mediate viral small RNA biogenesis and DNA virus induced silencing. Nucleic Acids Res. 2006;34(21):6233–46. https://doi.org/10.1093/nar/gkl886.
Bruce G, Gu M, Shi NN, Liu YL, Hong YG. Influence of retinoblastoma-related gene silencing on the initiation of DNA replication by African cassava mosaic virus Rep in cells of mature leaves in *Nicotiana benthamiana* plants. Virol J. 2011;8:561. https://doi.org/10.1186/1743-422X-8-561.
Chen WW, Zhang X, Fan YY, Li B, Ryabov E, Shi NN, et al. A genetic network for systemic RNA silencing in plant. Plant Physiol. 2018;176(4):2700–19. https://doi.org/10.1104/pp.17.01828.
Csorba T, Kontra L, Burgyán J. Viral silencing suppressors: tools forged to fine-tune host-pathogen coexistence. Virology. 2015;479–480:85–103. https://doi.org/10.1016/j.virol.2015.02.028.
Dadami E, Boutla A, Vrettos N, Tzortzakaki S, Karakasilioti I, Kalantidis K. DICER-LIKE 4 but not DICER-LIKE 2 may have a positive effect on potato spindle tuber viroid accumulation in *Nicotiana benthamiana*. Mol Plant. 2013;6(1):232–4. https://doi.org/10.1093/mp/sss118.
Dalakouras A, Dadami E, Wassenegger M. Engineering viroid resistance. Viruses. 2015;7(2):634–46. https://doi.org/10.3390/v7020634.
Daròs JA. *Eggplant latent viroid*: a friendly experimental system in the family *Avsunviroidae*. Mol Plant Pathol. 2016;17(8):1170–7. https://doi.org/10.1111/mpp.12358.
Di Serio F, Flores R, Verhoeven JTJ, Li SF, Pallás V, Randles JW, et al. Current status of viroid taxonomy. Arch Virol. 2014;159(12):3467–78. https://doi.org/10.1007/s00705-014-2200-6.
Di Serio F, Gisel A, Navarro B, Delgado S, Martínez de Alba AE, Donvito G, et al. Deep sequencing of the small RNAs derived from two symptomatic variants of a chloroplastic viroid: Implications for their genesis and for pathogenesis. PLoS ONE. 2009;4(10):7539. https://doi.org/10.1371/journal.pone.0007539.
Fadda Z, Daròs JA, Fagoaga C, Flores R, Duran-Vila N. Eggplant latent viroid, the candidate type species for a new genus within the family Avsunviroidae (hammerhead viroids). J Virol. 2003;77(11):6528–32. https://doi.org/10.1128/jvi.77.11.6528-6532.2003.
Flores R, Hernández C, Martínez de Alba AE, Daròs JA, Di Serio F. Viroids and viroid-host interactions. Annu Rev Phytopathol. 2005;43:117–39. https://doi.org/10.1146/annurev.phyto.43.040204.140243.
Gómez G, Pallás V. Noncoding RNA mediated traffic of foreign mRNA into chloroplasts reveals a novel signaling mechanism in plants. PLoS ONE. 2010;5(8): e12269. https://doi.org/10.1371/journal.pone.0012269.
Gómez G, Pallás V. Studies on subcellular compartmentalization of plant pathogenic noncoding RNAs give new insights into the intracellular RNA-traffic mechanisms. Plant Physiol. 2012;159(2):558–64. https://doi.org/10.1104/pp.112.195214.
Hadidi A, Flores R, Randles JW, Palukaitis P. Eds. Viroids and Satellites (Academic Press, London). 2017. https://www.sciencedirect.com/science/book/9780128014981.
Hamilton AJ, Baulcombe DC. A species of small antisense RNA in posttranscriptional gene silencing in plants. Science. 1999;286(5441):950–2. https://doi.org/10.1126/science.286.5441.950.
Jiang DM, Wang M, Li SF, Zhang ZX. High-throughput sequencing analysis of small RNAs derived from Coleus blumei viroids. Viruses. 2019;11(7):619. https://doi.org/10.3390/v11070619.
Katsarou K, Mavrothalassiti E, Dermauw W, Van Leeuwen T, Kalantidis K. Combined activity of DCL2 and DCL3 is crucial in the defense against potato spindle tuber viroid. PLoS Pathog. 2016;12(10): e1005936. https://doi.org/10.1371/journal.ppat.1005936.
Kovalskaya N, Hammond RW. Molecular biology of viroid-host interactions and disease control strategies. Plant Sci. 2014;228:48–60. https://doi.org/10.1016/j.plantsci.2014.05.006.
Kunnimalaiyaan M, Nielsen BL. Fine mapping of replication origins (Ori A and Ori B) in *Nicotiana tabacum* chloroplast DNA. Nucleic Acids Res. 1997;25(18):3681–6. https://doi.org/10.1093/nar/25.18.3681.
Langmead B, Salzberg SL. Fast gapped-read alignment with Bowtie 2. Nat Methods. 2012;9(4):357–9. https://doi.org/10.1038/nmeth.1923.
Li H, Handsaker B, Wysoker A, Fennell T, Ruan J, Homer N, et al. The sequence alignment/map format and SAMtools. Bioinformatics. 2009;25(16):2078–9. https://doi.org/10.1093/bioinformatics/btp352.
Liu SR, Zhou JJ, Hu CG, Wei CL, Zhang JZ. MicroRNA-mediated gene silencing in plant defense and viral counter-defense. Front Microbiol. 2017;8:1801. https://doi.org/10.3389/fmicb.2017.01801.
Mohamed A, Jin Z, Osman T, Shi N, Tör M, Jackson S, et al. Hotspot siRNA confers plant resistance against viral infection. Biology. 2022;11(5):714. https://doi.org/10.3390/biology11050714.
Martín R, Arenas C, Daròs JA, Covarrubias A, Reyes JL, Chua NH. Characterization of small RNAs derived from *Citrus exocortis viroid* (CEVd) in infected tomato plants. Virology. 2007;367(1):135–46. https://doi.org/10.1016/j.virol.2007.05.011.
Martínez de Alba AE, Flores R, Hernandez C. Two chloroplastic viroids induce the accumulation of small RNAs associated with posttranscriptional gene

silencing. J Virol. 2002;76(24):13094–6. https://doi.org/10.1128/jvi.76.24.13094-13096.2002.
Martínez F, Marquès J, Salvador ML, Daròs JA. Mutational analysis of eggplant latent viroid RNA processing in *Chlamydomonas reinhardtii* chloroplast. J Gen Virol. 2009;90(12):3057–65. https://doi.org/10.1099/vir.0.013425-0.
Martínez G, Donaire L, Llave C, Pallás V, Gómez G. High-throughput sequencing of Hop stunt viroid-derived small RNAs from cucumber leaves and phloem. Mol Plant Pathol. 2010;11(3):347–59. https://doi.org/10.1111/j.1364-3703.2009.00608.x.
Molina-Serrano D, Suay L, Salvador ML, Flores R, Daròs JA. Processing of RNAs of the family *Avsunviroidae* in *Chlamydomonas reinhardtii* chloroplasts. J Virol. 2007;81(8):4363–6. https://doi.org/10.1128/JVI.02556-06.
Nakasugi K, Crowhurst R, Bally J, Waterhouse P. Combining transcriptome assemblies from multiple de novo assemblers in the allo-tetraploid plant *Nicotiana benthamiana*. PLoS ONE. 2014;9(3): e91776. https://doi.org/10.1371/journal.pone.0091776.
Nakasugi K, Crowhurst RN, Bally J, Wood CC, Hellens RP, Waterhouse PM. De novo transcriptome sequence assembly and analysis of RNA silencing genes of *Nicotiana benthamiana*. PLoS ONE. 2013;8(3): e59534. https://doi.org/10.1371/journal.pone.0059534.
Navarro JA, Darós JA, Flores R. Complexes containing both polarity strands of avocado sunblotch viroid: identification in chloroplasts and characterization. Virology. 1999;253(1):77–85. https://doi.org/10.1006/viro.1998.9497.
Nohales MÁ, Molina-Serrano D, Flores R, Daròs JA. Involvement of the chloroplastic isoform of tRNA ligase in the replication of viroids belonging to the family *Avsunviroidae*. J Virol. 2012;86(15):8269–76. https://doi.org/10.1128/JVI.00629-12.
Pandey SP, Shahi P, Gase K, Baldwin IT. Herbivory-induced changes in the small-RNA transcriptome and phytohormone signaling in *Nicotiana attenuata*. Proc Natl Acad Sci USA. 2008;105(12):4559–64. https://doi.org/10.1073/pnas.0711363105.
Qin C, Li B, Fan YY, Zhang X, Yu ZM, Ryabov E, et al. Roles of Dicer-Like proteins 2 and 4 in intra- and intercellular Antiviral Silencing. Plant Physiol. 2017;174(2):1067–81. https://doi.org/10.1104/pp.17.00475.
Rao ALN, Kalantidis K. Virus-associated small satellite RNAs and viroids display similarities in their replication strategies. Virology. 2015;479–480:627–36. https://doi.org/10.1016/j.virol.2015.02.018.
Sarkies P, Miska EA. Small RNAs break out: the molecular cell biology of mobile small RNAs. Nat Rev Mol Cell Biol. 2014;15(8):525–35. https://doi.org/10.1038/nrm3840.
Shi Y, Gu M, Fan ZF, Hong YG. RNA silencing suppressors: how viruses fight back. Future Virol. 2008;3(2):125–33. https://doi.org/10.2217/17460794.3.2.125.
Shinozaki K, Sugiura M. Sequence of the intercistronic region between the ribulose-1, 5-bisphosphate carboxylase/oxygenase large subunit and coupling factor beta subunit gene. Nucleic Acids Res. 1982;10(16):4923–34. https://doi.org/10.1093/nar/10.16.4923.
Simón-Mateo C, García JA. MicroRNA-guided processing impairs Plum pox virus replication, but the virus readily evolves to escape this silencing mechanism. J Virol. 2006;80(5):2429–36. https://doi.org/10.1128/JVI.80.5.2429-2436.2006.
St-Pierre P, Hassen F, Thompson D, Perreault JP. Characterization of the siRNAs associated with peach latent mosaic viroid infection. Virology. 2009;383(2):178–82. https://doi.org/10.1016/j.virol.2008.11.008.
van Wezel R, Hong YG. Virus survival of RNA silencing without deploying protein-mediated suppression in *Nicotiana benthamiana*. FEBS Lett. 2004;562(1–3):65–70. https://doi.org/10.1016/S0014-5793(04)00184-X.
Wang MB, Bian XY, Wu LM, Liu LX, Smith NA, Isenegger D, et al. On the role of RNA silencing in the pathogenicity and evolution of viroids and viral satellites. Proc Natl Acad Sci USA. 2004;101(9):3275–80. https://doi.org/10.1073/pnas.0400104101.
Wang L, Yu X, Wang H, Lu YZ, de Ruiter M, Prins M, et al. A novel class of heat-responsive small RNAs derived from the chloroplast genome of Chinese cabbage (*Brassica rapa*). BMC Genomics. 2011;12:289. https://doi.org/10.1186/1471-2164-12-289.
Wang YJ, Gong Q, Jin ZH, Liu YL, Hong YG. Linking calcium and RNAi signaling in plants. Trends Plant Sci. 2022;27(4):328–30. https://doi.org/10.1016/j.tplants.2022.01.002.
Xu GY, Sui N, Tang Y, Xie K, Lai YZ, Liu YL. One-step, zero-background ligation-independent cloning intron-containing hairpin RNA constructs for RNAi in plants. New Phytol. 2010;187(1):240–50. https://doi.org/10.1111/j.1469-8137.2010.03253.x.
Yu ZM, Chen QY, Chen WW, Zhang X, Mei FL, Zhang PC, et al. Multigene editing via CRISPR/Cas9 guided by a single-sgRNA seed in *Arabidopsis*. J Integr Plant Biol. 2018;60(5):376–81. https://doi.org/10.1111/jipb.12622.
Zhang X, Lai TF, Zhang PC, Zhang XLA, Yuan C, Jin ZH, et al. Mini review: Revisiting mobile RNA silencing in plants. Plant Sci. 2019;278:113–7. https://doi.org/10.1016/j.plantsci.2018.10.025.
Zhang ZX, Qi SS, Tang N, Zhang XX, Chen SS, Zhu PF, et al. Discovery of replicating circular RNAs by RNA-seq and computational algorithms. PLoS Pathog. 2014;10(12): e1004553. https://doi.org/10.1371/journal.ppat.1004553.